

International Journal of Global Environmental Issues

ISSN online: 1741-5136 - ISSN print: 1466-6650

https://www.inderscience.com/ijgenvi

Investigating landslide susceptibility in the mountainous area of Union Territory Jammu and Kashmir, India: a comparative perspective

Lucky Sharma, Narendra Kumar Rana, Gaggan Kumar

DOI: <u>10.1504/IJGENVI.2024.10064539</u>

Article History:

Received: 30 January 2024 Last revised: 06 February 2024 Accepted: 01 April 2024

Published online: 26 September 2024

Investigating landslide susceptibility in the mountainous area of Union Territory Jammu and Kashmir, India: a comparative perspective

Lucky Sharma and Narendra Kumar Rana

Department of Geography, Institute of Science, Banaras Hindu University, Varanasi, Uttar Pradesh, 221005, India Email: lucky@bhu.ac.in

Email: imlucky1512@gmail.com Email: nkrana.in@gmail.com

Gaggan Kumar*

Department of Geography, Bhaderwah Campus, University of Jammu, 182222, India Email: gagan99geographer@gmail.com

*Corresponding author

Abstract: The escalation of geo-hazards, particularly landslides, has become a pressing concern, exacerbated by both natural factors and human activities. The frequency of rainfall-triggered landslides in mountainous regions is surging, posing imminent threats to lives and infrastructure. Jammu and Kashmir witness this peril throughout the year, affecting millions. This study focuses on creating a landslide susceptibility map for District Doda, employing a multi-method approach. A comparative analysis of multi-criteria decision method-analytical hierarchy process (AHP) and Shannon information entropy (SIE) determines their efficacy. The inventory, comprising 250 landslides, incorporates nine conditioning factors. AHP designates 91% of the area as very high or highly susceptible, while SIE identifies 46.49% as vulnerable. Area under curve (AUC) values of 0.898 and 0.976 for AHP and SIE, respectively, underscore the latter's superior predictive capability. This study is instrumental in aiding stakeholders with decision-making, land-use planning, and formulating effective mitigation strategies.

Keywords: landslide; susceptibility; Shannon entropy; analytical hierarchy process; AHP; geohazards; decision-making.

Reference to this paper should be made as follows: Sharma, L., Rana, N.K. and Kumar, G. (2024) 'Investigating landslide susceptibility in the mountainous area of Union Territory Jammu and Kashmir, India: a comparative perspective', *Int. J. Global Environmental Issues*, Vol. 23, No. 1, pp.23–46.

Biographical notes: Lucky Sharma belongs to Jammu, UT of Jammu and Kashmir, India. He qualified his Master's in Science in Geography from University of Jammu. He is currently pursuing his PhD in Geography from Banaras Hindu University, Varanasi under supervision of Dr. Narendra Kumar Rana. He is currently working in the field of disaster management.

Narendra Kumar Rana is currently a Professor in the Department of Geography, Institute of Science, Banaras Hindu University, Varanasi, India. He received his Master's and MPhil from Delhi University and PhD from Deen Dayal Upadhyaya Gorakhpur University, Gorakhpur. He is presently working on environmental hazards, vulnerability and risk assessment and river restoration.

Gaggan Kumar is currently designated as an Assistant Professor in Department of Geography, in Government Degree College of Women, Kathua associated with University of Jammu. He completed his PhD from University of Jammu. He has also held a Lecturer position in Offside campus of University of Jammu for four years in Bhaderwah. He has also written several papers in associated field and currently working in geomorphology and climate change.

1 Introduction

Growing frequency of anthropogenic activities like expanding transportation infrastructure, building dams and growing cities in ecologically fragile regions have accelerated the frequency of natural hazards and their repercussions (Kumar and Anbalagan, 2016; GNDAR, 2021). According to the prediction of UNDRR (2022) report, there will be 560 human casualties by 2023 due to natural hazards triggering more economic losses. Among various geo-hazards landslides represent a serious hazard in many areas of the world (Guzzetti et al., 2012). A 'landslide' is the movement of a mass of rock, debris or earth down a slope under the impact of gravity (Cruden and Varnes, 1996) and transported material is mostly weathered rock slide (Hungr et al., 2001). Subaerial and subaqueous landslides are also possible, and a variety of natural occurrences, such as prolonged or strong rainfall, earthquakes, fast snowmelt, volcanic activity, and several human acts, can all result in landslides (Cruden and Varnes, 1996) as well as the frequency of landslides has increased by 3%, causing enormous damage to infrastructure and human life (GNDAR, 2021; El Jazouli et al., 2019). Topographic factors like geology, groundwater characteristics, slope, curvature, land use, pedology (Kumar and Anbalagan, 2016; Van Westen et al., 2008) and triggering factors like rainfall, earthquakes and over-anthropocentrism (Lazzari and Piccarreta, 2018; Ray et al., 2009; Sultana, 2020) are also known to have contributed in amplifying the impacts of landslides. Landslides are more prevalent in mountainous regions around the world, and they pose a hazard to the communities that live there as well as other infrastructure like railroads and roadways (Pandey et al., 2019; Wu et al., 2020). The natural surface runoff process and slope continuity have been altered by the changing mountainous landscape, which includes a shrinking forest landscape, an increase in urban settlements, and a pacing up of the provision of transportation facilities, that have raised the threat of landslides (Chuang and Shiu, 2018; Mcoll, 2022).

Indian Himalayas are prone to landslides triggered by torrential rain and earthquakes. Owing to hilly and varied topography, frequent escarpment, faults and pulverised rocks, the landslide-driven hazards have been become more frequent and disastrous especially during the monsoon season (Kumar et al., 2017; Martha et al., 2021). Few excerpts of events from Himalayas such as Sadal Village Landslide (Kumar et al., 2017), Assar landslide (Singh et al., 2012), Pawari Landslide zone (Kumar et al., 2018), Lanta Khola landslide (Anbarasu et al., 2010) indicate the activeness of landslide hazard intimidating the population, exposing communication and transport infrastructure to great loss. A recent study also indicated the North West Himalayas are the most fatal in terms of landslide (Parkash, 2011).

Thus, it is necessary to understand the landslide susceptibility of a region like India Himalayas because the evolution, development process and susceptibility of landslide assessment are labyrinthine. Previous literature revealed that there are different quantitative, qualitative, semi quantitative and deterministic model for the landslide susceptibility assessment (Dikshit et al., 2020). Landslide susceptibility often deals with spatial distribution of probability of occurrence of landslide considering the conditioning factors (Reichenbach et al., 2018). Landslide zonation remained vital for the developmental activities in understanding the topographical factors (Pandey et al., 2020). Landslide susceptibility mapping have been conducted using multi criteria method (Intarawichian and Dasananda, 2010; Kumar and Anbalagan, 2016), frequency ratio (Ding et al., 2017; Addis, 2023), Gaussian theorem (Gao et al., 2022), weight of evidence (Ilia and Tsangaratos, 2016; Getachew and Meten, 2021), machine learning algorithm like support vector machine (Pandey et al., 2020, Ballabio and Sterlacchini, 2012), boosted regression tree (Pandey et al., 2019, Saha et al., 2021), random forest (Hong et al., 2016, Park and Kim, 2019), index of entropy method (Pourghasemi et al., 2012; Wubalem et al., 2022) and many more. Various techniques come with their own set of limitations. For example, machine learning methods may not be dependable for broad user due to their stringent criteria and the need for powerful computing system. Multivariate statistical approaches struggle to assess the contribution of individual classes (Wubalem and Meten, 2020). Nevertheless, bivariate statistical methods offer a promising solution as they can yield favourable results by pinpointing the class contribution and are relatively straightforward to manage (Wubalem, 2021). Amongst all the bivariate method, frequency ratio (FR) along with index of entropy method is widely utilised, although requires previous landslide data (Wubalem et al., 2022). Presence of previous landslide database poses no restriction in carrying out this study.

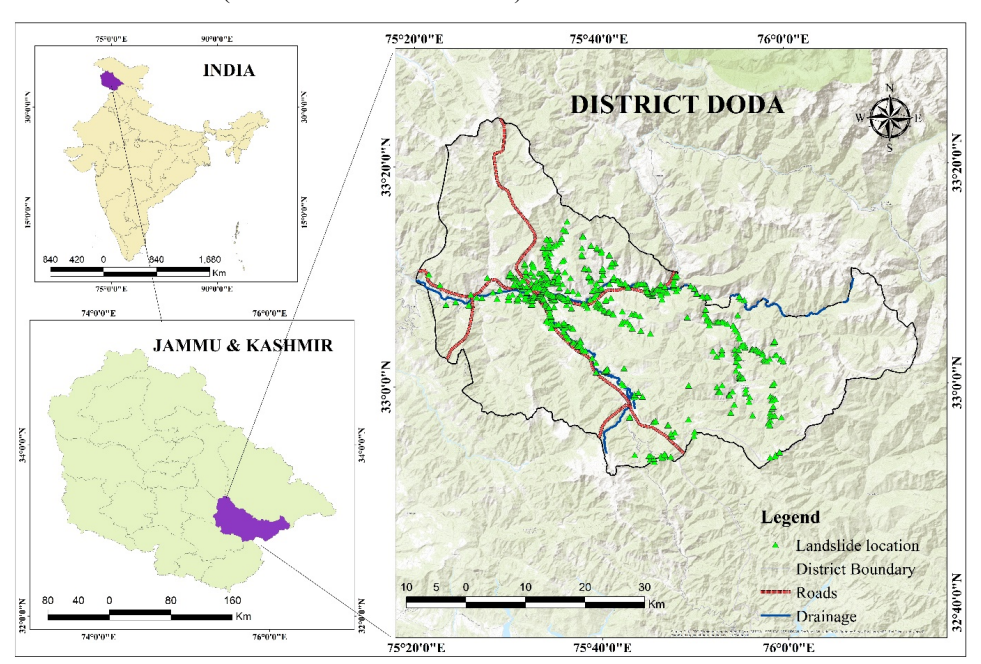
Dikshit et al. (2020) in their analysis of the research gap revealed that Jammu and Kashmir along with North Eastern states lacked the research in this particular sub-field of enquiry that is landslide susceptibility. According to Shah et al. (2022), there is decadal increase in the number of landslides from 136 to 373, severely affecting villagers and commuters depriving them of basic necessities for a few days. He also reported that Ramban (38), Kishtwar (34) and Doda (32) have the highest frequency of death totalling to 1,000 death in the region. He also observed that landslides occur more frequently in the winter season than in the monsoon. Ali et al. (2022) have also observed those landslides are the major secondary disaster during the monsoon along the National Highways isolating the Kashmir Valley from the rest of the India. Thus, the Jammu and Kashmir experience landslide not only in monsoon but in winters as well. It becomes imperative as researcher to fill the gap and study the landslide susceptibility in the area

having region's one of the highest causalities. To carry out this objective in an area having dearth of studies on comparative approach, analytical hierarchy process and FR-Shannon entropy method have been compared and duly validated to check their prediction.

2 Study area

One of the mountainous districts of Jammu division of Union Territory of Jammu and Kashmir (UT of J&K) is Doda lying in the south eastern part of the region in the Middle Himalayas (as shown in Figure 1). The geographical extent lies between 320 51' to 330 24' latitude and 750 20' to 760 14' longitude having a total area of 2,408 sq. km. It is surrounded by Kishtwar on the East and North East, Udhampur on the South West and Kathua in the South, Anantnag in the North and Ramban in the North West. The area spans across lush green forest, delicate geology, beautiful valleys and glaciers. The climate varies is subhumid temperate type in the study area (Rashid et al., 2013). The region had a long history of landslides which Singh et al. (2012) elaborated how one slide detached one district from accessing resources. Presence of Muree thrust and Panjal thrust (shown as fault in Figure 2) is also one of the main concerns that on shaking brittle rocks nearby broke down into pieces (Singh et al., 2012). Patel et al. (2020) reviewed that 2009 landslide detached the whole district by disrupting the road linkages and spiked the food prices for a month due to stranding vehicles on the roads.

Figure 1 Map of the study area showing national highways, major river system and historical landslides (see online version for colours)



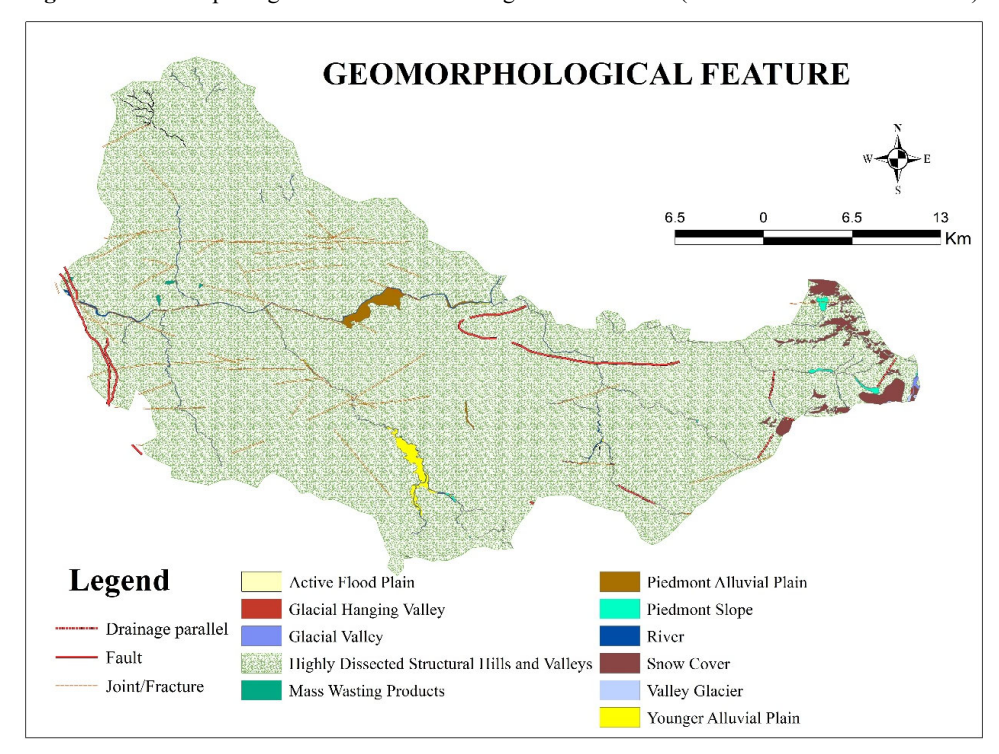


Figure 2 Geomorphological feature shown along with lineaments (see online version for colours)

3 Methods and materials

3.1 Data sources

The secondary data has been used for conducting the study (as shown in the Table 1). The Shuttle Radar Topography Mission Digital Elevation Model (SRTM DEM) was used which was downloaded from US Geological Survey (USGS) Earth Explorer having resolution 30 metres. The IMD gridded data of resolution (0.5 * 0.5 degree) was utilised for showing rainfall. The geological data was downloaded from the BHUKOSH, the web portal of Geological Survey of India. The OSM database was also utilised for downloading road network. The satellite data like Sentinel-2, Landsat 8 OLI/ TRS and Gridded Soil database of National Oceanic and Atmospheric Administration (NOAA) was also utilised in this study.

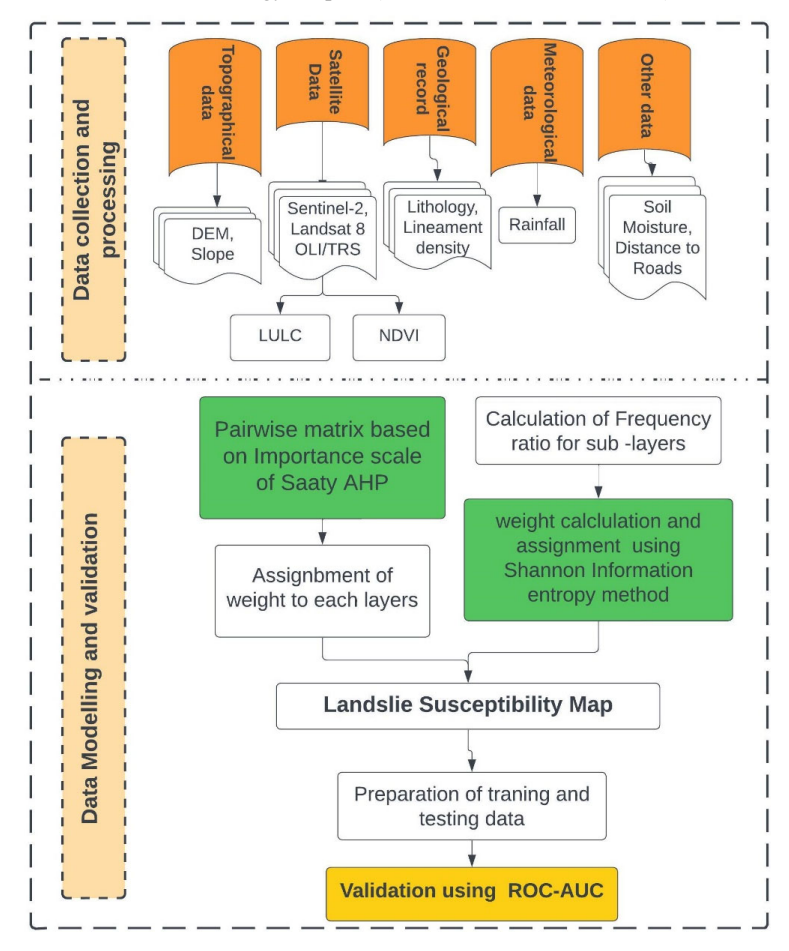
3.2 Methodology

The methodology adopted for the present study is discussed below and is also shown in Figure 3.

 Table 1
 The conditioning parameter causing landslide

S. no.	PARAMETERS	SOURCE
1	ELEVATION	SRTM DEM (30 m) downloaded from USGS EARTH EXPLORER
2	SLOPE	Derived from SRTM DEM
3	LAND USE LAND COVER	SENTINEL 2 Satellite imagery, resolution 10 m
4	LITHOLOGY	BHUKOSH portal, Geological Survey of India
5	LINEAMENT DENSITY	BHUKOSH portal, Geological Survey of India
6	SOIL MOISTURE	Gridded soil Database, NOAA, USA (0.5*0.5 degree)
7	NDVI	Landsat 8 OLI/TRS, 30 m resolution
8	RAINFALL	IMD gridded data (0.5*0.5 degree)
9	Distance to roads	OSM Database

Figure 3 Flowchart of methodology adopted (see online version for colours)



3.2.1 Preparation of inventory of landslide causing conditioning factors

The formation of inventory is, indeed, the preliminary stage for the landslide assessment to be conducted as it involves data collection and its processing (Zhou et al., 2018). The study prepared the inventory by adopting three methods: historical data from the Geological Survey of India (2015 and above), imageries from Google Earth followed by field investigation. We carefully considered 625 landslides occurred in the study area since 2015 for the evaluation and analysing their relationship with causing factors. The different conditioning factors have been identified based on previous literature and the availability of data (Süzen and Kaya, 2012) which are as shown in Table 1.

3.2.1.1 Elevation

Elevation is a significant conditioning factor derived from the SRTM DEM having resolution 30 m. Ranging between 695 m to 4,956 m, at lower elevation, the risk of landslide remains less pronounced (Intarawichian and Dasananda, 2010) [Figure 4(a)].

3.2.1.2 Slope

The major targeting factor amongst the topographic factors in landslide assessment is slope (Nourani et al., 2014) which is derived from the SRTM DEM in ArcGIS. The slope angle map was classified into five classes at an interval of 150 ranging from 00 to 74.210. Raising slope angle results in increased shear strength, which decreases slope stability, enhanced the likelihood of landslide in general (Çellek, 2020) [Figure 4(b)].

3.2.1.3 Lineament density

Lineament is generally an expression of geological feature like fault in an area (Arifin and Adnan, 2021). The possibility of landslides near the lineament is sufficiently high as the strength to hold the rock during the tectonic movement become weak (Chen et al., 2017). The lineaments in line format were downloaded from the BHUKOSH, a web-portal of Geological Survey of India. The density map is prepared by using linear density tool of the spatial analyst tool [Figure 4(c)]. Ranging from 0 to 11.11 km, the lineament density is highest near the river flowing through the area.

3.2.1.4 Rainfall

It is considered as a triggering factor whose impact is widely known. Rainfall data was collected from the Indian Meteorological Department in gridded format and further processed to form the rainfall map. High rainfall influencing the runoff affects slope stability and relates to higher occurrence of landslide in space time context (Bui et al., 2011). The rainfall ranged from 797 mm to 1,224 mm [Figure 4(h)] showing the enhancing susceptibility.

3.2.1.5 Soil moisture

Soil moisture substantially impacts the occurrence of landslide by increasing the runoff and enhanced erosion (Fayaz and Khader, 2020). Soil moisture map [Figure 4(e)] is prepared from the data downloaded in the gridded (0.5*0.5 degrees) format from NOAA,

USA. It ranged from 357 to 363 mm showing higher susceptibility in the parts having higher soil moisture.

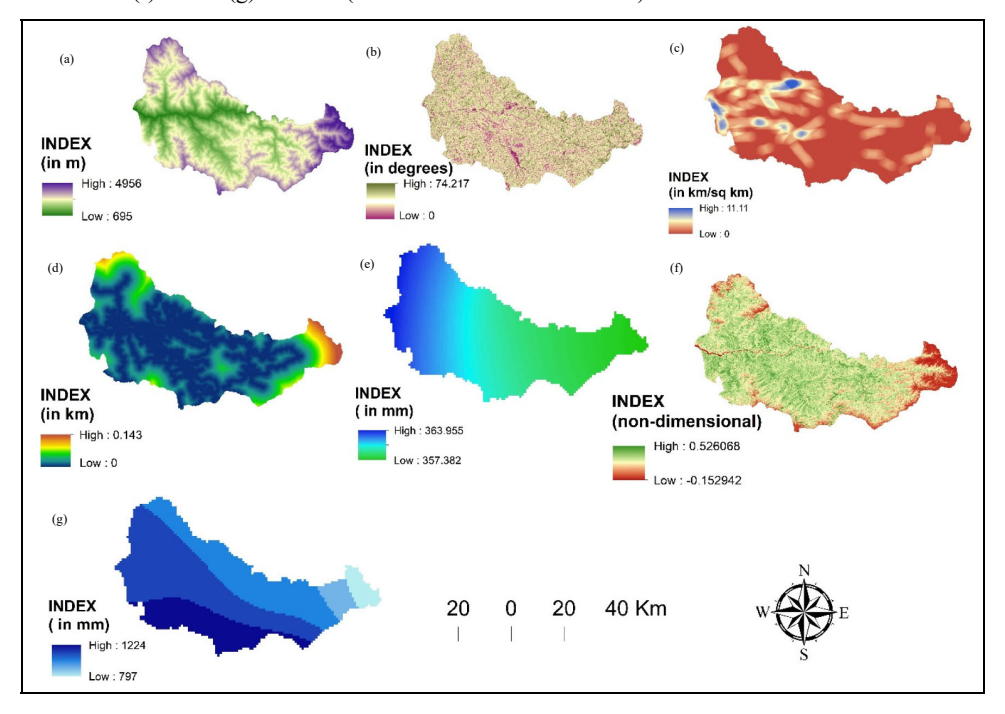
3.2.1.6 Normalised difference vegetative index (NDVI)

The function of vegetation is indispensable as it maintains soil structure and reduces the risk of landslide (Peduzzi, 2010). Thus, NDVI is considered and mapped using the Landsat 8 OLI/TRS satellite image. NDVI is prepared using the following formula

$$NDVI = (Band 5 - Band 4)/(Band 5 + Band 4)$$
 (1)

The value of NDVI ranged from -0.152 to 0.526 [Figure 4(f)] revealing less potential of landslide in higher NDVI values.

Figure 4 (a) Elevation (b) Slope (c) Lineament density (d) Distance to roads (e) Soil moisture (f) NDVI (g) Rainfall (see online version for colours)



3.2.1.7 Distance to roads

This factor is substantial in assessing the risk of landslide hazard as human activities like transportation facilities have greatly influenced the geological structure and milieu (Guo et al., 2019). Road network is downloaded from OpenStreetMap (OSM) database and the distance to road [Figure 4(d)] is prepared from the Euclidean distance tool in ArcGIS software with an interval of 30 m.

3.2.1.8 Lithology

It is another compelling factor in addition to slope because variation in lithological feature often produces substantial differences in permeability and strength of the rock (Pradhan et al., 2010). Lithology map [Figure 5(b)] was prepared after downloading from the BHUKOSH, a web-portal of Geological Survey of India. We identified 23 different formations but the carbonaceous phyllite with marble and quartzite is dominant in the central part of the area followed by carbonaceous slate with phyllite and leucratic to mesocratic biotite granite.

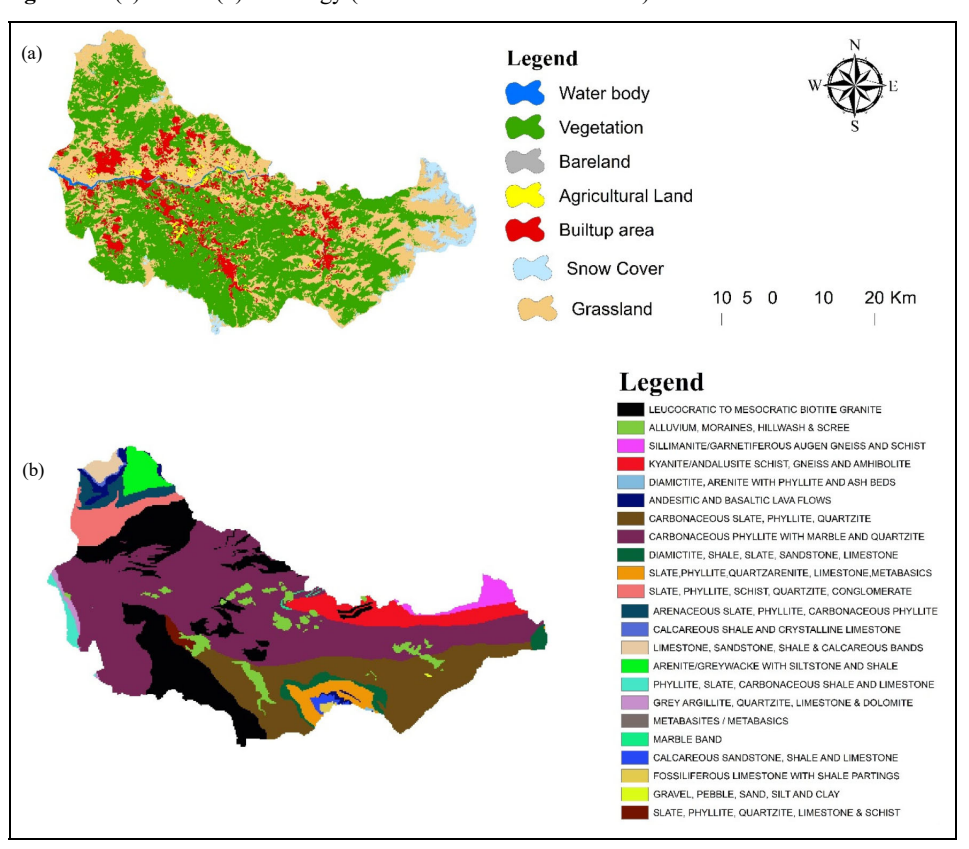
Table 2 Geology age and lithology in the study area

S. no.	Lithology	Formation	Group	Age
1	Leucocratic to mesocratic biotite granite	Kaplas Granite/ Kazinag/Hant/ Pipra*		Palaeozoic
2	Alluvium, moraines, hillwash and scree		Undifferentiated quaternary	Pleistocene to Holocene
3	Biotite gneiss and quartz/garnetiferous mica schist	Sangra and Parkachik (Undiff)	Gaimbal = Suru crystalline	Palaeoproterozoic
4	Sillimanite/garnetiferous augen gneiss and schist	Parkachik	Gaimbal = Suru crystalline	Palaeoproterozoic
5	Kyanite/andalusite schist, gneiss and amhibolite	Sangra	Gaimbal = Suru crystalline	Palaeoproterozoic
6	Diamictite, arenite with phyllite and ash beds	Agglomeratic Slate	Pir Panjal	Late Carboniferous to Early Permian
7	Andesitic and basaltic lava flows	Panjal Volcanics	Pir Panjal	Permian
8	Carbonaceous slate, phyllite, quartzite	Chamba	Vaikrita	Proterozoic (Undiff)
9	Carbonaceous phyllite with marble and quartzite	Salkhala		Proterozoic (Undiff)
10	Diamictite, shale, slate, sandstone, limestone	Manjir = Langera		Neoproterozoic
11	Slate, Phyllite, quartzarenite, limestone, metabasics	Katarigali		Neoproterozoic
12	Slate, phyllite, schist, quartzite, conglomerate	Ramsu	Hapatnar	Neoproterozoic
13	Arenaceous slate, phyllite, carbonaceous phyllite	Machhal	Hapatnar	Neoproterozoic
14	Calcareous shale and crystalline limestone	Zewan	Vihi	Late Permian
15	Limestone, sandstone, shale and calcareous bands	Khunamuh, Khreuh and Wuyan (Undiff)	Vihi	Permian to Triassic
16	Arenite/Greywacke with siltstone and shale	Lolab	Pohru = Sind	Cambrian

 Table 2
 Geology age and lithology in the study area (continued)

S. no.	Lithology	Formation	Group	Age
17	Phyllite, slate, carbonaceous shale and limestone	Ramban		Neoproterozoic
18	Grey argillite, quartzite, limestone and dolomite	Sincha		Neoproterozoic
19	Metabasites/metabasics	Salkhala		Proterozoic (Undiff)
20	Marble band	Salkhala		Proterozoic (Undiff)
21	Calcareous sandstone, shale and limestone	Salooni, Kukti, Gamgul	Tandi	Permian to Jurassic
22	Fossiliferous limestone with shale partings	Dalman		Triassic
23	Gravel, pebble, sand, silt and clay		Undifferentiated quaternary	Pleistocene to Holocene
24	Slate, phyllite, quartzite, limestone and schist	Bhaderwah		Neoproterozoic

Figure 5 (a) LULC (b) Lithology (see online version for colours)



3.2.1.9 Land use land cover

Land use land cover (LULC) represents a decisive conditioning factor that increase or decrease the risk of any hazard (Kanungo et al., 2006). It was prepared using Sentinel-2 satellite image having 10 m resolution and was classified into seven classes: waterbody, vegetation, grassland, agricultural land, snow cover, barren land and built-up area [Figure 5(a)].

3.2.2 Application of analytical hierarchy process-multicriteria decision method

Multicriteria decision method is a common approach in hazard monitoring in which analytical hierarchy process (AHP) is widely used for evaluating criteria based on importance scale (Table 3) and identifying weights. It is Saaty in the year 1980s who developed this approach. This approach entails expert participation and orientation for comparing between the criteria keeping objective at the top. This approach involved a preparation of pairwise matrix table of criteria and computation of normalised weights. The consistency ratio is finally computed for accuracy check which is found to be less than 10%.

Consistency index (CI) =
$$\frac{\lambda_{\text{max}} - 1}{n - 1}$$
 (2)

Consistency ratio (CR) =
$$CI/RI$$
 (3)

whereas RI – random index (shown in Table 4).

Table 3 Importance scale given by Saaty (1980)

S. no.		Explanation						Intensity of relative importance			
1		In case	of criteria	A and B	are equal	ly importa	ınt	1			
2	In case of criteria A is moderately important than B								3		
3	In case of criteria A is strongly important than B						5				
4	In case of criteria A is very strongly important than B						7				
5	In case of criteria A is extremely important than B						9				
6	In case of intermediate judgements							2,4,6,8			
Гable 4	Ra	ındom in	dex as giv	en by Saa	aty						
N	1	2	3	4	5	6	7	8	9	10	
RI	0	0	0.52	0.89	1 12	1 26	1.36	1 41	1 46	1.49	

3.2.3 Application of Shannon information entropy method

For objective based weight assigning methods, Claude Shannon happened to have propounded the information entropy theory (Shannon, 1948; Lianxiao and Morimoto, 2019). In this study, frequency ratio (FR) was first calculated using following formulas:

$$FR = \frac{\frac{\text{No. of pixel of landslide in class}}{\text{No. of total pixel in class}}}{\frac{\text{No. of total pixel in class}}{\text{total landslide pixel in class}}}$$
(4)

Entropy is calculated using FR of each class present in layer utilising following equations.

The specific gravity V_{ij} , among the n indices of the i^{th} evaluation item of the index, j is as follows:

$$V_{ij} = \frac{Y'_{ij}}{\sum_{i=1}^{n} Y'_{ij}}$$
 (5)

Among Y' is the frequency ratio calculated using equation (4).

Information entropy is calculated using E_i is as follows:

$$E_{j} = -K \sum_{i=1}^{n} V_{ij} * ln(V_{ij})$$
(6)

whereas $k = 1/\ln(n)$, assured when $V_{ij} = 0$, $\ln(V_{ij}) = 0$.

Utility value D_i for index j is calculated as follows:

$$D_{i} = 1 - E_{i} \tag{7}$$

in which the entropy value E_i is higher, smaller value D_i is calculated.

The weight of each layer is calculated using following equation:

$$W_{j} = D_{j} / \sum D_{j}$$
 (8)

3.2.4 Constructing landslide hazard vulnerability map

After evaluating the weight of all thematic layers, they were overlayed to prepare landslide vulnerability map by utilising following formula:

$$LHVM = \sum_{i=1}^{n} w_i * H_i$$

whereas w_i – weight of respective layer and H_i – classified conditioning layer.

3.2.5 Validation using area under receiver operating characteristic

For validating the final landslide map, area under receiver operating characteristic (AU-ROC) curve was utilised to observe the accuracy of the map by comparing the landslide inventory map and AHP and Shannon information entropy (SIE)-based final map. El Jazouli et al. (2019) discussed in detail the importance and role of AU-ROC curve in prediction. ROC curve is frequently used curve to estimate the probability of occurrence of events. AU-ROC curve value range from 0 to 1 in which values above 0.6 are considered satisfactory and values above 0.8 and 0.9 represents the good and excellent predictive value. In this study, we took 250 landslide and non-landslide points

utilising the imagery and field methodology and divided the data into 70% training dataset and 30% testing dataset randomly for the validation.

4 Results

4.1 Analysis of historical database

The landslides have previously devastated the study area with its frequent occurrence. A look at Table 5 revealed the movement, types and their distribution. Debris slide and rock cum debris slide have dominantly stressed the area accounting for 78% of the previous occurrence. Their movement was shallow translational in nature. Out of the considered landslides, 41.87% showed advancing and 54.14% possessed retrogressive distribution.

Table 5 Types, movement as well as the distribution of historical landslides

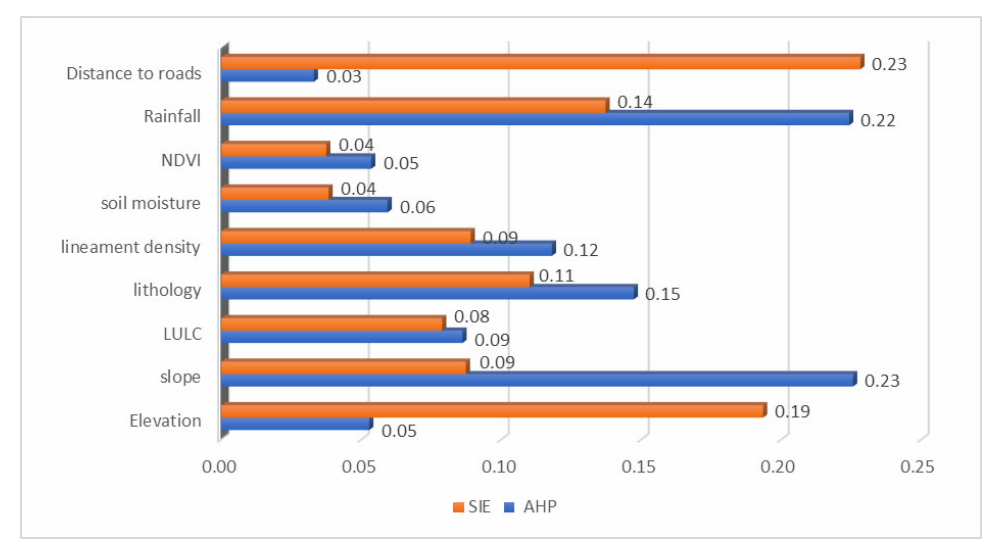
S. no.	Description	Percentage
	Types of landslides	S
1	Rock cum debris fall	1.07
2	Rock fall	7.06
3	Debris fall	0.61
4	Rock cum debris slide	25.92
5	Rock slide	11.35
6	Debris slide	52.61
7	Composite rock slide	1.38
	Types of movement	t
1	Shallow translation	98.01
2	Deep translational	1.99
	Types of distribution	n
1	Advancing	41.87
2	Advancing and retrogressive	0.31
3	Confined	0.15
4	Enlarging	1.53
5	Retrogressive	54.14
6	Widening	1.99

4.2 Contribution of conditioning factors

Estimating the contribution of factors and subfactors is a significant step in removing the irrelevant input and improving the accuracy of predicting ability of a model (Pourghasemi et al., 2021). Both AHP and SIE approaches were applied in this investigation to calculate their contribution in affecting landslides. Utilising AHP, slope, rainfall, lithology and lineament density were determined to have significantly higher contribution in generating the landslide susceptibility map (LSM) (as shown in Figure 6)

whereas in case of SIE, distance to roads, rainfall, elevation, lithology and slope were contributing maximum in creation of LSM.

Figure 6 Predictive capabilities of individual factors computed by AHP and SIE (see online version for colours)



In addition, the weights for layers and sub-layers of the factors are as much significant for improving the LSM that are computed and are shown in Tables 6 and 7. The consistency ration for AHP pairwise matrix was found to be 0.922.

 Table 6
 Pairwise matrix computed for conditioning factors

	EL	SL	LULC	Li	LD	SM	NDVI	R	DTR	NW
EL	1.00	0.20	0.33	0.17	1.00	2.00	0.50	0.20	2.00	0.05
SL	5.00	1.00	4.00	2.00	1.00	2.00	5.00	2.00	5.00	0.23
LULC	3.00	0.25	1.00	1.00	1.00	1.00	1.00	0.50	2.00	0.09
Li	6.00	0.50	1.00	1.00	1.00	3.00	5.00	0.33	5.00	0.15
LD	1.00	1.00	1.00	1.00	1.00	3.00	3.00	0.33	4.00	0.12
SM	0.50	0.50	1.00	0.33	0.33	1.00	2.00	0.20	2.00	0.06
NDVI	2.00	0.20	1.00	0.20	0.33	0.50	1.00	0.20	3.00	0.05
R	5.00	0.50	2.00	3.00	3.00	5.00	5.00	1.00	3.00	0.22
DTR	0.50	0.20	0.50	0.20	0.25	0.50	0.33	0.33	1.00	0.03

 $\label{eq:noise_energy} Note: EL-\ elevation, SL-\ slope, Li-\ lithology, LD-\ lineament\ density, SM-\ soil\\ moisture, R-\ rainfall, DTR-\ distance\ to\ roads, NW-\ normalised\ weights.$

 Table 7
 Weights computed for sub layers of conditioning factors

S. no.	Layers	Sub-layers	Percentage of area under class	Percentage of area under landslides	Weights (AHP)	Weights (entropy)			
1	Lithology	Leucocratic to mesocratic biotite granite	16.934	7.400	0.045	0.046			
		Alluvium, moraines, hillwash and scree	3.166	4.175	0.119	0.138			
		Sillimanite/garnetiferous augen gneiss and schist	1.583	0.000	0.024	0.000			
		Kyanite/andalusite schist, gneiss and amhibolite	5.118	4.554	0.049	0.093			
		Diamictite, arenite with phyllite and ash beds	0.035	0.000	0.026	0.000			
		Andesitic and basaltic lava flows	1.105	0.000	0.026	0.000			
		Carbonaceous slate, phyllite, quartzite	16.611	13.852	0.049	0.087			
		Carbonaceous phyllite with marble and quartzite	40.571	67.742	0.076	0.175			
		Diamictite, shale, slate, sandstone, limestone	1.917	1.328	0.052	0.073			
		Slate, phyllite, quartzarenite, limestone, metabasics	2.240	0.380	0.052	0.018			
		Slate, phyllite, schist, quartzite, conglomerate	3.449	0.000	0.026	0.000			
		Arenaceous slate, phyllite, carbonaceous phyllite	1.954	0.000	0.026	0.000			
		Calcareous shale and crystalline limestone	0.175	0.000	0.026	0.000			
		Limestone, sandstone, shale and calcareous bands	0.851	0.000	0.026	0.000			
						Arenite/greywacke with siltstone and shale	1.975	0.000	0.026
		Phyllite, slate, carbonaceous shale and limestone	0.655	0.000	0.026	0.000			
		Grey argillite, quartzite, limestone and dolomite	0.457	0.000	0.026	0.000			
		Metabasites/metabasics	0.004	0.000	0.027	0.000			
		Marble band	0.100	0.190	0.132	0.198			
		Calcareous sandstone, shale and limestone	0.363	0.190	0.062	0.055			
		Fossiliferous limestone with shale partings	0.169	0.190	0.130	0.118			

 Table 7
 Weights computed for sub layers of conditioning factors (continued)

S. no.	Layers	Sub-layers	Percentage of area under class	Percentage of area under landslides	Weights (AHP)	Weights (entropy)
		Gravel, pebble, sand, silt and clay	0.023	0.000	0.026	0.000
		Slate, phyllite, quartzite, limestone and schist	0.544	0.000	0.026	0.000
2	Slope	0–14	8.659	1.905	0.062	0.058
		14–28	39.911	26.984	0.097	0.179
		28-40	42.011	56.984	0.160	0.358
		40–56	9.221	14.127	0.263	0.405
		56–74	0.197	0.000	0.419	0.000
3	Elevation	695–1,609	13.353	59.206	0.046	0.770
		1,609–2,213	34.013	32.540	0.096	0.166
		2,213-2,788	34.954	5.397	0.136	0.027
		2,788-3,513	13.524	2.857	0.256	0.037
		3,513-4,956	4.156	0.000	0.466	0.000
4	Rainfall	797–926	4.337	0.000	0.045	0.000
		926-1,013	4.681	0.000	0.079	0.000
		1,013-1,074	29.146	33.446	0.144	0.396
		1,074–1,127	42.925	59.797	0.262	0.481
		1,127–1,224	18.910	6.757	0.470	0.123
5	NDVI	(-0.15)-0.05	9.166	3.175	0.071	0.073
		0.05-0.015	28.900	45.238	0.430	0.331
		0.015-0.22	14.214	24.127	0.148	0.359
		0.22-0.28	33.085	19.206	0.225	0.123
		0.28-0.52	14.635	8.254	0.125	0.119
6	LULC	Waterbody	0.506	1.429	0.042	0.223
		Vegetation	51.752	2.143	0.049	0.003
		Agricultural land	1.348	4.821	0.180	0.283
		Built up area	9.374	36.607	0.105	0.309
		Bareland	0.594	0.357	0.324	0.048
		Snow cover	3.437	0.179	0.044	0.004
		Grassland	32.988	54.464	0.255	0.131
7	Lineamen	0–2.2	59.141	84.393	0.471	0.501
	t density	2.2–4.4	25.803	9.827	0.268	0.134
		4.4–6.6	10.679	3.083	0.143	0.101
		6.6–8.8	3.583	2.697	0.075	0.264
		8.8–11.1	0.795	0.000	0.044	0.000

S. no.	Layers	Sub-layers	Percentage of area under class	Percentage of area under landslides	Weights (AHP)	Weights (entropy)
8	Distance	0-1.1	50.301	92.293	0.471	0.844
	to roads	1.1-2.8	28.672	6.744	0.268	0.108
		2.8-5.2	10.315	0.771	0.143	0.034
		5.2-8.8	6.600	0.193	0.075	0.013
		8.8-14.3	4.111	0.000	0.044	0.000
9	Soil	353.58-358.59	24.786	23.333	0.044	0.192
	moisture	358.77–359.77	22.026	23.000	0.075	0.213
		359.77-361.01	18.971	37.000	0.143	0.399
		361.01-362.27	17.631	13.333	0.268	0.155
		362.27-363.95	16.586	3.333	0.471	0.041

 Table 7
 Weights computed for sub layers of conditioning factors (continued)

4.3 Landslide susceptibility assessment

The modelling results indicated that LSM generated from AHP and SIE (as shown in Figure 7) have been categorised into five based on natural break method: very low, low, moderate, high and very high susceptibility. The AHP model indicated that 83.33% and 8.6% of the area come under high and very high susceptibility class respectively. The SIE model indicated that 20.79%, 25.74%, 17.74%, 22.52%, and 13.20% of Doda District fell under very high, high, moderate, low and very low classes respectively. The area under different classes computed by both methods is shown in Figure 8. It is significant to note that only 46% of the area was falling under high and very high susceptibility classes in SIE approach which accounted for 1,120 sq. km of the total study area whereas total of 2,000 sq. km was falling under high landslide susceptibility. The very high and high susceptibility areas were found in the central part of the study area in proximity to river and roads and heavy concentration of built-up area.

4.4 Spatial relationship between factors and landslide

An attempt is made to decipher the spatial relationship between factors and the landslide in the district Doda. The relationship was understood through factors and classes of LSM falling under the high and very high susceptibility. It was understood that occurrence of landslide was highly recorded in the elevation between 1,609–2,788 m whereas in between 609–1,609 m, very high susceptibility was also observed by SIE. The slope of 140 to 400 was coincided with high susceptibility to landslides. Majority of the landslides fell under the rainfall of 1,013 m to 1,224 m in the study area. It was noticed that calcareous phyllite with marble and quartzite formation along with fossiliferous limestone with shale partings and alluvium, moraine, hill wash and scree were the major formation predisposed to landslides. Major land use like agricultural land, built up area, grassland and bare land were prone to landslide. Not only this, NDVI ranging between 0.05 to 0.28 revealed the high occurrence of landslides in the study area. Soil moisture,

distance to roads and lineament density revealed the decreasing trend in the values showing the occurrence of landslides.

Figure 7 Landslide susceptibility map using (a) AHP and (b) SIE (see online version for colours)

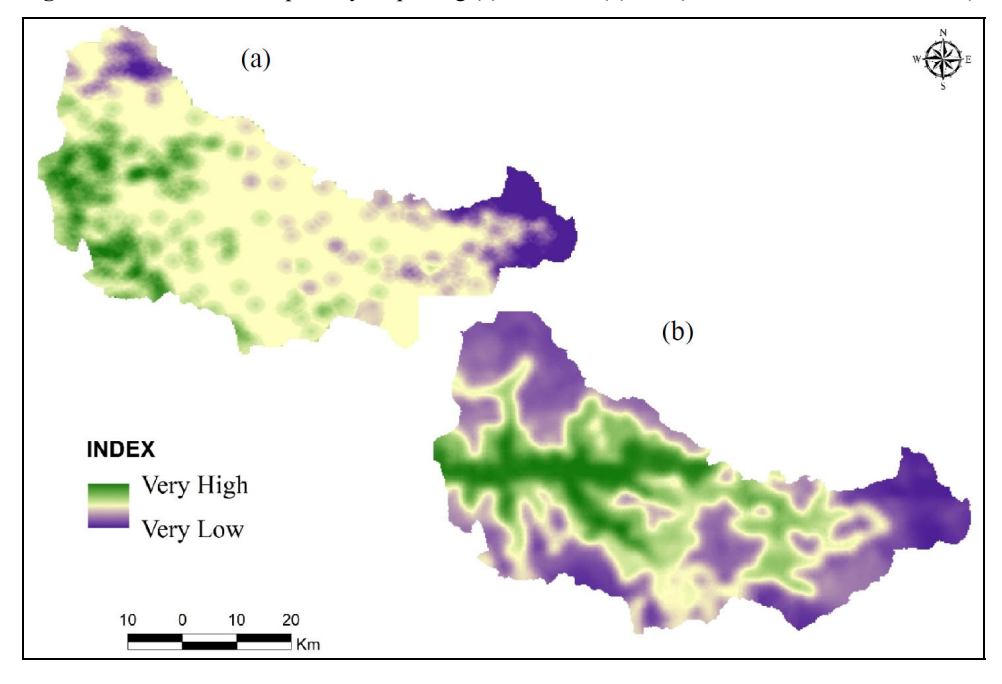
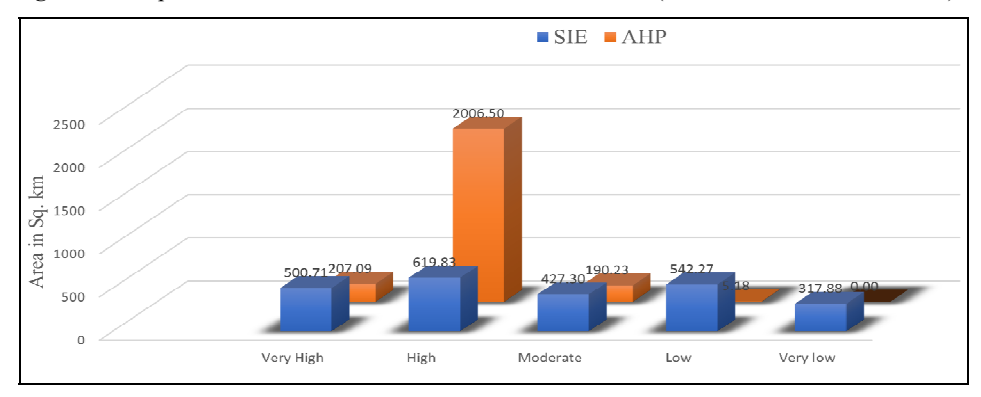


Figure 8 Proportion of area under the different landslide classes (see online version for colours)



4.5 Validation

No study is completed until it is validated. In this study, validation of output LSM map was evaluated using AU-ROC curve (as shown in Figure 9) which indicated that value of AU-ROC curve for AHP was 0.898 and for SIE was 0.976. The value of curve showed that predictive ability of maps under AHP and SIW was good for the both the models. Through the curve, SIE method was best fit among the two to represent landslide hazard zone map.

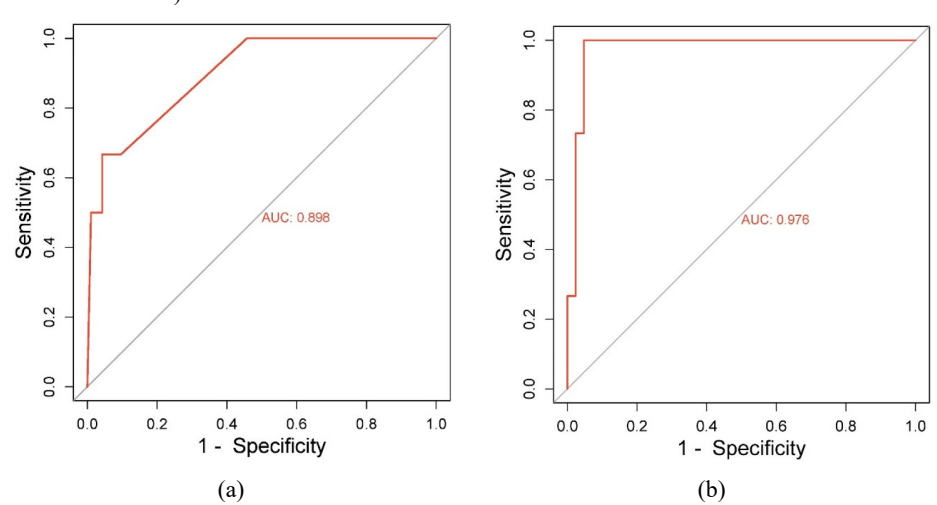


Figure 9 (a) validation curve for AHP (b) Validation curve for SIE (see online version for colours)

5 Discussion

Multitude of studies has carried out on landslide susceptibility assessment using comparative approach involving multi criteria with statistical analysis, within different machine learning algorithm, or combining machine learning algorithm with statistical analysis to find out the best fit method (Chen et al., 2017; Ding et al., 2017; Pandey et al., 2020). In the present attempt, we incorporated the multi criteria AHP and Shannon information entropy method to evaluate the best approach among them since Shannon entropy has never utilised in such comparative study. This study revealed that around 45% of study area was comprised of landslide prone area as per SIE approach when validated found in excellent category as per area under curve whereas 83.33% of area found highly vulnerable in accordance with AHP approach. This huge difference was attributed to subjectivity bias of multi criteria method and dominance of weights of slope, rainfall and lithology computed by AHP enhancing the inconsistency in the results. The findings revealed that mainly lower slope, higher rainfall, moderate elevation along with closer distance to roads and fault were the major determinants in the occurrences of the landslides. The weak lithological nature of the region exhibiting carbonaceous phyllite with marble, carbonaceous slate with phyllite underneath the low vegetation section of the region have enhanced the likelihood of landslide. The understanding can be gained from the weak lithology that how the intrusion of construction activities along this lithological bed could threaten the area. El Jazouli et al. (2019) had even considered slope, lithology and distance to lineament as the major causative factors but distance to road as well as land use could have a triggering impact and have had the potential to activate the landslide under the definite condition. The insights can be gained from the study of Singh et al. (2012) that the slide in the study area was induced due to construction of the reservoir. Another factor included was soil moisture owing to the reason cited by the study conducted by Singh et al. (2012), stated that rock had poor absorption capacity. The study was quite in contrast to Singh et al. (2012) as it found the high susceptible region in 140 to 400 slopes whereas another study by Kumar et al. (2017) explains this fact that clay and sandstone have weakness at 100 to 400 towards slope failure. The computed results provided the highest weight to 'distance to road' under SIE approach which can be proved through the excerpt from the Patel et al. (2020) review study stating that the 2009 landslide on NH 1B road impacted many lives by blocking the road and enhancing the food security problem over a month. The rainfall, which has been found the major determinant under both the methods, cannot be ignored being the major triggering factor as Kumar et al. (2017) established the strong relationship between the rainfall and occurrence of landslide.

It is concluded from the results that the SIE have the better capability because of utilisation of contribution of each conditioning factor using the past location of landslide which is not possible in AHP. The computed value of AUC has found to be higher than the performance of machine learning algorithms, i.e., 0.976 authenticating the SIE model as one of the best fitted models. The insight from Ding et al. (2017) and Pourghasemi et al. (2021) displayed the average value of AUC to be 0.900 proving the worth of the study. The difference of 7.8

% in between the performance of the model was attributed to larger portion of higher area under high susceptibility under AHP method. The study had even gained an advantage from historical database of national government that helped in improving the results of study.

The primary drawback of the study is that downscaling and upscaling of the available data, as few sources have higher scale, could have exacerbated the discrepancies in the findings. Furthermore, the study's future potential lies in evaluating soil physical and chemical attributes, which would enhance its ability to make predictions about the future.

6 Conclusions

Since the frequency of landslides is surging every year, the mountainous landscape is changing abruptly owing to rainfall induced landslides in alliance with increased human interventions. This study aimed to investigate the susceptibility of landscape through the comparative perspective involving analytical hierarchical process and Shannon information entropy models. The study evidenced that Shannon entropy approach is a good predictor of likelihood of landslide computing 46% of the total area under high and very high susceptibility whose performance is validated using AUC value. The analysis found rainfall, slope, lithology, distance to roads and lineament to be the major conditioning factors contributing to occurrences of landslides. Major occurrences were located in proximity to the roads, and stream endangering the concentrated built-up area on the slopes. The outcome will provide insights to the disaster response team to prepare for evacuation process. It will aid in restricting the future construction activities in the very high and high susceptibility zones. The strategy of reforestation can have huge impact in preventing the future landslides. Furthermore, construction of retaining wall and avoiding overloading of slopes should be adopted to prevent excess soil erosion and mishap from forthcoming disaster. Lastly, this study will also support stakeholders in decision making, land use planning and formulating mitigation strategies for taking prompt action.

References

- Addis, A. (2023) 'GIS-based landslide susceptibility mapping using frequency ratio and Shannon entropy models in Dejen District, Northwestern Ethiopia', *Journal of Engineering*, Vol. 2023, Article ID 1062388.
- Ali, N., Alam, A., Bhat, M.S. and Shah, B. (2022) 'Using historical data for developing a hazard and disaster profile of the Kashmir valley for the period 1900–2020', *Natural Hazards*, Vol. 114, No. 2, pp.1609–1646.
- Anbarasu, K., Sengupta, A., Gupta, S. and Sharma, S.P. (2010) 'Mechanism of activation of the Lanta Khola landslide in Sikkim Himalayas', *Landslides*, Vol. 7, No. 2, pp.135–147.
- Arifin, A. and Adnan, N.A. (2021) 'Geological lineament assessment from passive and active remote sensing imageries', *International Journal of Geospatial and Environmental Research*, Vol. 8, No. 2, p.5.
- Ballabio, C. and Sterlacchini, S. (2012) 'Support vector machines for landslide susceptibility mapping: the Staffora River Basin case study, Italy', *Mathematical Geosciences*, Vol. 44, pp.47–70.
- Bui, D.T., Lofman, O., Revhaug, I. and Dick, O. (2011) 'Landslide susceptibility analysis in the Hoa Binh province of Vietnam using statistical index and logistic regression', *Nat Hazards*, Vol. 59, No. 3, pp.1413–1444.
- Çellek, S. (2020) 'Effect of the slope angle and its classification on landslide', *Natural Hazards and Earth System Sciences Discussions*, pp.1–23, https://doi.org/10.21203/rs.3.rs-61660/v1.
- Chen, W., Xie, X., Wang, J., Pradhan, B., Hong, H., Bui, D.T., Duan, Z. and Ma, J., (2017) 'A comparative study of logistic model tree, random forest, and classification and regression tree models for spatial prediction of landslide susceptibility', *Catena*, Vol. 151, No. 1, pp.147–160.
- Chuang, Y.C. and Shiu, Y.S. (2018) 'Relationship between landslides and mountain development integrating geospatial statistics and a new long-term database', *Science of the Total Environment*, Vol. 622, pp.1265–1276, https://doi.org/10.1016/j.scitotenv.2017.12.039.
- Cruden, D.M. and Varnes, D.J. (1996) 'Landslide types and processes', in Turner, A.K. and Schuster, R.L. (Eds.): *Landslides, Investigation and Mitigation*, Special Report 247, pp.36–75, Transportation Research Board, Washington DC, ISSN: 0360-859X, ISBN: 030906208X.
- Dikshit, A., Sarkar, R., Pradhan, B., Segoni, S. and Alamri, A.M. (2020) 'Rainfall induced landslide studies in Indian Himalayan region: a critical review', *Applied Sciences*, Vol. 10, No. 7, p.2466.
- Ding, Q., Chen, W. and Hong, H. (2017) 'Application of frequency ratio, weights of evidence and evidential belief function models in landslide susceptibility mapping', *Geocarto International*, Vol. 32, No. 6, pp.619–639.
- El Jazouli, A., Barakat, A. and Khellouk, R. (2019) 'GIS-multicriteria evaluation using AHP for landslide susceptibility mapping in Oum Er Rbia high basin (Morocco)', *Geoenvironmental Disasters*, Vol. 6, No. 1, pp.1–12.
- Fayaz, M. and Khader, S.A. (2020) 'Identifying the parameters responsible for Landslides on NH-44 Jammu Srinagar National Highway for Early Warning System', *Disaster Advances*, Vol. 13, No. 2, pp.32–42.
- Gao, Z., Ding, M., Huang, T., Liu, X., Hao, Z., Hu, X. and Chuanjie, X. (2022) 'Landslide risk assessment of high-mountain settlements using Gaussian process classification combined with improved weight-based generalized objective function', *International Journal of Disaster Risk Reduction*, Vol. 67, No. 1, p.102662.
- Getachew, N. and Meten, M. (2021) 'Weights of evidence modeling for landslide susceptibility mapping of Kabi-Gebro Locality, Gundomeskel Area, Central Ethiopia', *Geoenvironmental Disasters*, Vol. 8, No. 1, pp.1–22.
- GNDAR (2021) Global Natural Disaster Assessment Report, International Federation of Red Cross and Red Crescent Societies, National Disaster Reduction Centre of China, Academy of

- Disaster Reduction and Emergency Management [online] https://www.preventionweb.net/publication/2020-global-natural-disaster-assessment-report (accessed 26 June 2023).
- Guo, C., Qin, Y., Ma, D., Xia, Y., Chen, Y., Si, Q. and Lu, L. (2019) 'Ionic composition, geological signature and environmental impacts of coalbed methane produced water in China', *Energy Sources, Part A: Recovery, Utilization, and Environmental Effects*, Vol. 43, No. 10, pp.1–15.
- Guzzetti, F., Mondini, A.C., Cardinali, M., Fiorucci, F., Santangelo, M. and Chang, K.T. (2012) 'Landslide inventory maps: new tools for an old problem', *Earth-Science Reviews*, Vol. 112, Nos. 1–2, pp.42–66.
- Hong, H., Pourghasemi, H.R. and Pourtaghi, Z.S. (2016) 'Landslide susceptibility assessment in Lianhua County (China): a comparison between a random forest data mining technique and bivariate and multivariate statistical models', *Geomorphology*, Vol. 259, pp.105–118.
- Hungr, O., Evans, S.G., Bovis, M.J. and Hutchinson, J.N. (2001) 'A review of the classification of landslides of the flow type', *Environmental & Engineering Geoscience*, Vol. 7, No. 3, pp.221–238, https://doi.org/10.2113/gseegeosci.7.3.221.
- Ilia, I. and Tsangaratos, P. (2016) 'Applying weight of evidence method and sensitivity analysis to produce a landslide susceptibility map', *Landslides*, Vol. 13, No. 2, pp.379–397.
- Intarawichian, N. and Dasananda, S. (2010) 'Analytical hierarchy process for landslide susceptibility mapping in Lower Mae Chaem Watershed, Northern Thailand', *Suranaree Journal of Science & Technology*, Vol. 17, No. 3, pp.1–16.
- Kanungo, D.P., Arora, M.K., Sarkar, S. and Gupta, R.P. (2006) 'A comparative study of conventional, ANN black box, fuzzy and combined neural and fuzzy weighting procedures for landslide susceptibility zonation in Darjeeling Himalayas', *Engineering Geology*, Vol. 85, Nos. 3–4, pp.347–366.
- Kumar, A., Asthana, A.K.L., Priyanka, R.S., Jayangondaperumal, R., Gupta, A.K. and Bhakuni, S.S. (2017) 'Assessment of landslide hazards induced by extreme rainfall event in Jammu and Kashmir Himalaya, Northwest India', Geomorphology, Vol. 284, pp.72–87, https://doi.org/10.1016/j.geomorph.2017.01.003.
- Kumar, R. and Anbalagan, R. (2016) 'Landslide susceptibility mapping using analytical hierarchy process (AHP) in Tehri reservoir rim region, Uttarakhand', *Journal of the Geological Society of India*, Vol. 87, No. 3, pp.271–286.
- Kumar, V., Gupta, V. and Jamir, I. (2018) 'Hazard evaluation of progressive Pawari landslide zone, Satluj Valley, Himachal Pradesh, India', *Natural Hazards*, Vol. 93, No. 2, pp.1029–1047.
- Lazzari, M. and Piccarreta, M. (2018) 'Landslide disasters triggered by extreme rainfall events: the case of Montescaglioso (Basilicata, Southern Italy)', *Geosciences*, Vol. 8, No. 10, p.377.
- Lianxiao and Morimoto, T. (2019) 'Spatial analysis of social vulnerability to floods based on the MOVE framework and information entropy method: case study of Katsushika Ward, Tokyo', *Sustainability*, Vol. 11, No. 2, p.529.
- Martha, T.R., Roy, P., Jain, N., Khanna, K., Mrinalni, K., Kumar, K.V. and Rao, P.V.N. (2021) 'Geospatial landslide inventory of India – an insight into occurrence and exposure on a national scale', *Landslides*, Vol. 18, No. 6, pp.2125–2141, https://doi.org/10.1007/s10346-021-01645-1.
- Mcoll, S.T. (2022) 'Landslide causes and triggers', *Landslide Hazards, Risks, and Disasters*, 2nd ed., Chapter 2, pp.13–41, Elsevier, ISBN 9780128184646, https://doi.org/10.1016/B978-0-12-818464-6.00011-1.
- Nourani, V., Baghanam, A.H., Adamowski, J. and Kisi, O. (2014) 'Applications of hybrid wavelet-artificial intelligence models in hydrology: a review', *Journal of Hydrology*, Vol. 514, No. 1, pp.358–377.
- Pandey, V.K., Pourghasemi, H.R. and Sharma, M.C. (2020) 'Landslide susceptibility mapping using maximum entropy and support vector machine models along the Highway Corridor, Garhwal Himalaya', *Geocarto International*, Vol. 35, No. 2, pp.168–187.

- Pandey, V.K., Sharma, K.K., Pourghasemi, H.R. and Bandooni, S.K. (2019) 'Sedimentological characteristics and application of machine learning techniques for landslide susceptibility modelling along the highway corridor Nahan to Rajgarh (Himachal Pradesh), India', *Catena*, Vol. 182, No. 1, p.104150.
- Park, S. and Kim, J. (2019) 'Landslide susceptibility mapping based on random forest and boosted regression tree models, and a comparison of their performance', *Applied Sciences*, Vol. 9, No. 5, p.942.
- Parkash, S. (2011) 'Historical records of socio-economically significant landslides in India', Journal of South Asia Disaster Studies, Vol. 4, No. 2, pp.177–204.
- Patel, S.K., Nanda, A., Singh, G. and Patel, S. (2020) 'A review of disasters in Jammu and Kashmir, and Ladakh region in India', *International Journal of Population Studies*, Vol. 6, No. 1, pp.69–81, DOI: 10.18063/ijps.v6i1.1180/.
- Peduzzi, P. (2010) 'Landslides and vegetation cover in the 2005 North Pakistan earthquake: a GIS and statistical quantitative approach', *Natural Hazards and Earth System Sciences*, Vol. 10, No. 4, pp.623–640.
- Pourghasemi, H.R., Mohammady, M. and Pradhan, B. (2012) 'Landslide susceptibility mapping using index of entropy and conditional probability models in GIS: Safarood Basin, Iran', *Catena*, Vol. 97, No. 11, pp.71–84.
- Pourghasemi, H.R., Sadhasivam, N., Amiri, M., Eskandari, S. and Santosh, M. (2021) 'Landslide susceptibility assessment and mapping using state-of-the art machine learning techniques', *Natural Hazards*, Vol. 108, No. 1, pp.1291–1316.
- Pradhan, B., Lee, S. and Buchroithner, M.F. (2010) 'Remote sensing and GIS-based landslide susceptibility analysis and its cross-validation in three test areas using a frequency ratio model', *Photogrammetrie-Fernerkundung-Geoinformation*, Vol. 1, No. 1, pp.17–32.
- Rashid, I., Romshoo, S.A. and Vijayalakshmi, T. (2013) 'Geospatial modelling approach for identifying disturbance regimes and biodiversity rich areas in North Western Himalayas, India', *Biodiversity and Conservation*, Vol. 22, No. 13, pp.2537–2566.
- Ray, P.C., Parvaiz, I., Jayangondaperumal, R., Thakur, V.C., Dadhwal, V.K. and Bhat, F.A. (2009) 'Analysis of seismicity-induced landslides due to the 8 October 2005 earthquake in Kashmir Himalaya', *Current Science*, Vol. 97, No. 12, pp.1742–1751.
- Reichenbach, P., Rossi, M., Malamud, B.D., Mihir, M. and Guzzetti, F. (2018) 'A review of statistically-based landslide susceptibility models', *Earth-Science Reviews*, Vol. 180, No. 1, pp.60–91.
- Saaty, T.L. (2008) 'Decision making with the analytic hierarchy process', *Int. J. Serv. Sci.*, Vol. 1, No. 1, pp.83–98.
- Saha, S., Arabameri, A., Saha, A., Blaschke, T., Ngo, P.T. T., Nhu, V.H. and Band, S.S. (2021) 'Prediction of landslide susceptibility in Rudraprayag, India using novel ensemble of conditional probability and boosted regression tree-based on cross-validation method', *Science* of the Total Environment, Vol. 764, No. 1, p.142928.
- Shah, B., Sultan Bhat, M., Alam, A., Sheikh, H.A. and Ali, N. (2022) 'Developing landslide hazard scenario using the historical events for the Kashmir Himalaya', *Natural Hazards*, Vol. 114, No. 3, pp.3763–3785.
- Shannon, C.E. (1948) 'A mathematical theory of communication', *The Bell System Technical Journal*, Vol. 27, No. 3, pp.379–423.
- Singh, Y., Bhat, G.M., Sharma, V., Pandita, S.K. and Thakur, K.K. (2012) 'Reservoir induced landslide at Assar, Jammu and Kashmir: a case study', *Journal of the Geological Society of India*, Vol. 80, No. 3, pp.435–439.
- Sonker, I., Tripathi, J.N. and Singh, A.K. (2021) 'Landslide susceptibility zonation using geospatial technique and analytical hierarchy process in Sikkim Himalaya', *Quaternary Science Advances*, Vol. 4, No. 1, p.100039, https://doi.org/10.1016/j.qsa.2021.100039.

- Sultana, N. (2020) 'Analysis of landslide-induced fatalities and injuries in Bangladesh: 2000–2018', Cogent Social Sciences, Vol. 6, No. 1, p.1737402, https://doi.org/10.1080/23311886.2020.1737402.
- Süzen, M.L. and Kaya, B.Ş. (2012) 'Evaluation of environmental parameters in logistic regression models for landslide susceptibility mapping', *International Journal of Digital Earth*, Vol. 5, No. 4, pp.338–355.
- United Nations Office for Disaster Risk Reduction (UNDRR) (2022) Global Assessment Report on Disaster Risk Reduction 2022: Our World at Risk: Transforming Governance for a Resilient Future, Geneva.
- Van Westen, C.J., Castellanos, E. and Kuriakose, S.L. (2008) 'Spatial data for landslide susceptibility, hazard, and vulnerability assessment: an overview', *Engineering Geology*, Vol. 102. Nos. 3–4, pp.112–131.
- Wu, R., Zhang, Y., Guo, C., Yang, Z., Tang, J. and Su, F. (2020) 'Landslide susceptibility assessment in mountainous area: a case study of Sichuan-Tibet railway, China', *Environmental Earth Sciences*, Vol. 79, No. 1, pp.1–16.
- Wubalem, A. (2021) 'Landslide susceptibility mapping using statistical methods in Uatzau catchment area, northwestern Ethiopia', *Geoenvironmental Disasters*, Vol. 8, No. 1, p.1.
- Wubalem, A. and Meten, M. (2020) 'Landslide susceptibility mapping using information value and logistic regression models in Goncha Siso Eneses area, northwestern Ethiopia', *SN Applied Sciences*, Vol. 2, No. 1, pp.1–19.
- Wubalem, A., Getahun, B., Hailemariam, Y., Mesele, A., Tesfaw, G., Dawit, Z. and Goshe, E. (2022) 'Landslide susceptibility modeling using the index of entropy and frequency ratio method from Nefas-Mewcha to Weldiya Road Corridor, Northwestern Ethiopia', *Geotechnical and Geological Engineering*, Vol. 40, No. 10, pp.5249–5278.
- Zhou, C., Yin, K., Cao, Y., Ahmed, B., Li, Y., Catani, F. and Pourghasemi, H.R. (2018) 'Landslide susceptibility modeling applying machine learning methods: a case study from Longju in the Three Gorges Reservoir area, China', *Computers & Geosciences*, Vol. 112, No. 1, pp.23–37.